HHS Public Access

Author manuscript

Arterioscler Thromb Vasc Biol. Author manuscript; available in PMC 2021 January 01.

Published in final edited form as:

Arterioscler Thromb Vasc Biol. 2020 January ; 40(1): 206–219. doi:10.1161/ATVBAHA.119.312771.

A novel autoimmune IgM antibody attenuates atherosclerosis in IgM deficient low fat diet-fed, but not Western diet-fed *Apoe*$^{-/-}$ mice

Olga A. Cherepanova[1,2,3,*], **Prasad Srikakulapu**[1], **Elizabeth S. Greene**[1], **Malay Chaklader**[3], **Ryan M. Haskins**[1,4], **Mary E. McCanna**[1], **Smarajit Bandyopadhyay**[5], **Bhupal Ban**[6,7,8], **Norbert Leitinger**[1,9], **Coleen A. McNamara**[1,10], **Gary K. Owens**[1,2,*]

[1]Robert M. Berne Cardiovascular Research Center, University of Virginia, Charlottesville, VA, USA

[2]Department of Molecular Physiology and Biological Physics, University of Virginia, Charlottesville, VA, USA

[3]Department of Cardiovascular and Metabolic Sciences, Lerner Research Institute, Cleveland Clinic, USA

[4]Department of Pathology, University of Virginia, Charlottesville, VA, USA

[5]Molecular Biotechnology Core, Research Core Services, Lerner Research Institute, Cleveland Clinic, USA

[6]Antibody Engineering and Technology Core, University of Virginia, USA

[7]Department of Cell Biology, University of Virginia, USA

[8]Indiana Biosciences Research Institute, USA

[9]Department of Pharmacology, University of Virginia, Charlottesville, VA, USA

[10]Cardiovascular Division, Department of Medicine, University of Virginia, Charlottesville, VA, USA

Abstract

Objective ––Oxidized phospholipids (OxPL), such as the oxidized derivatives of PAPC (1-palmitoyl-2-arachidonoyl-*sn*-glycero-3-phosphorylcholine), POVPC (1-palmitoyl-2-(5-oxovaleroyl)-*sn*-glycero-3-phosphorylcholine) and PGPC (1-palmitoyl-2-glutaroyl-*sn*-glycero-3-phosphorylcholine), have been shown to be the principal biologically active components of minimally oxidized LDL. The role of OxPL in cardiovascular diseases is well recognized, including activation of inflammation within vascular cells. Atherosclerotic *Apoe*$^{-/-}$ mice fed a high fat diet develop antibodies to OxPL, and hybridoma B-cell lines producing natural anti-OxPL

*Correspondence should be addressed to Dr. Olga A. Cherepanova (cherepol@ccf.org; phone: +1-216-445-7491) and Dr. Gary K. Owens (gko@virginia.edu, phone: +1-434-924-9173).

DISCLOSURES

None

Any Supplementary Information is available in the online version of the paper.

autoantibodies have been successfully generated and characterized. However, as yet, no studies have been reported demonstrating that treatment with OxPL neutralizing antibodies can be used to prevent or reverse advanced atherosclerosis.

Approach and Results ––Herein, using a screening against POVPC/PGPC we generated a novel IgM autoantibody, 10C12, from the spleens of *Apoe*$^{-/-}$ mice fed a long term Western diet, that demonstrated potent OxPL neutralizing activity *in vitro*, and the ability to inhibit macrophage accumulation within arteries of *Apoe*$^{-/-}$ mice fed a Western diet for four weeks. Of interest, 10C12 failed to inhibit atherosclerosis progression in *Apoe*$^{-/-}$ mice treated between 18-26 weeks of Western diet feeding likely due at least in part to high levels of endogenous anti-OxPL antibodies. However, 10C12 treatment caused a 40% decrease in lipid accumulation within aortas of secreted IgM deficient, *sIgM*$^{-/-}$*Apoe*$^{-/-}$, mice fed a low fat diet, when the antibody was administrated between 32-40 weeks of age.

Conclusions ––Taken together, these results provide the first direct evidence showing that treatment with a single autoimmune anti-OxPL IgM antibody during advanced disease stages can have an atheroprotective outcome.

Graphical Abstract

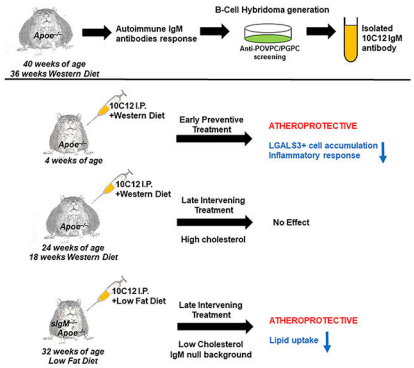

Keywords

POVPC; PGPC; natural autoantibody; atherosclerosis; IgM deficient mice; Animal Models of Human Disease; Lipids and Cholesterol

INTRODUCTION

Atherosclerosis is a chronic disease of the arterial wall which contributes to >40% of all deaths worldwide. Although its incidence in the USA has decreased modestly over the last decade, it is still the leading global cause of death and is expected to increase at a particularly rapid rate in the future. This increase is due to the increased westernization of the world and the accompanying worldwide obesity and type II diabetes epidemic, which are known to greatly exacerbate atherosclerosis pathogenesis. Lipid accumulation and oxidation within the arterial wall are the leading causes of atherosclerosis development and progression[1,2].

There is a growing body of evidence for the role of oxidized phospholipids (OxPL) as modulators of inflammatory processes[3]. These modified OxPL are derived from lipoproteins or cellular membranes and accumulate at sites of inflammation such as atherosclerotic lesions. Minimally modified Low Density Lipoprotein (LDL) is a major atherogenic factor, the biological activity of which is attributable to OxPL derived from PAPC (1-palmitoyl-2-arachodonoyl-*sn*-glycero-3-phosphorylcholine), forming POVPC (1-palmitoyl-2-(5-oxovaleroyl)-*sn*-glycero-3-phosphorylcholine) and PGPC (1-palmitoyl-2-glutaroyl-*sn*-glycero-3-phosphorylcholine). OxPL have been shown to influence a variety of cellular functions such as inflammatory cytokine/chemokine production and expression of adhesion molecules in endothelial cells and macrophages[4,5]. Moreover, previous studies in our laboratory demonstrated that OxPL induce profound phenotypic switching of vascular smooth muscle cells (SMC) including suppression of multiple SMC differentiation marker genes, increased migration and proliferation, and increased expression of genes implicated in plaque formation, remodeling, and/or stability including MCP1, MCP3, matrix metalloproteinases and collagens[6–9].

The presence of antibodies to phosphorylcholine OxPL in patients with atherosclerosis, diabetes, hypertension, antiphospholipid syndrome, preeclampsia, and other chronic diseases underlines the importance of these molecules as potential therapeutic targets in the treatment or prevention of multiple diseases[10–13]. Dr. Witztum's group discovered that extensive atherosclerosis in atheroprone *Apoe*$^{-/-}$ mice is associated with robust antibody titers to oxidized LDL (OxLDL)[14–17]. They were able to generate splenic hybridoma B-cell lines from these "naïve" mice, which produced monoclonal IgM autoantibodies to OxLDL, termed E0 antibodies[16]. Of major importance, sequencing the antigen binding sites of these antibodies showed that E0 IgMs are genetically and structurally indistinguishable from the T15 natural antibodies specific for phosphorylcholine that were identified over 30 years ago[18]. T15 antibodies were initially reported as the most protective antibody toward lethal systemic infection with *Streptococcus pneumoniae*, in which the phosphorylcholine is directly conjugated to the cell wall polysaccharide[19]. Further studies from Dr. Witztum's group showed that immunization of atheroprone *Ldlr*$^{-/-}$ mice with *Streptococcus pneumoniae* resulted in strong induction of IgM titers to OxLDL and reduced the progression of atherosclerosis[20], suggesting that an immune response to OxLDL might modulate atherogenesis. Another study from Dr. Haskard's group demonstrated that *Ldlr*$^{-/-}$ mice deficient in serum IgM displayed a substantial acceleration of aortic and aortic root atherosclerotic lesion formation on both low-fat and high-fat diets[21].

Of particular relevance, several different E0 antibodies that were selected on the basis of their binding to OxLDL were shown to recognize OxPL containing the phosphorylcholine headgroup, such as POVPC and PGPC[22,23]. Moreover, it has been shown that a POVPC/PGPC-recognizing E0 IgM antibody, E06, had a neutralizing effect *in vitro*[16,24,25]. Importantly, a recent study demonstrated that 1% high-cholesterol diet-fed *Ldlr*$^{-/-}$ mice expressing a single-chain variable fragment of E06 using the *Apoe* promoter (*Ldlr*$^{-/-}$ E06-scFv mice) had significantly less atherosclerosis, as well as a demonstrable decrease in systemic inflammation and a decrease in aortic valve calcification[26]. However, although together these data strongly suggest that phosphorylcholine OxPL are pro-atherogenic, there

is **no direct evidence** demonstrating that exogenous OxPL neutralizing antibody treatment can inhibit or reverse the development of established atherosclerotic lesions. Indeed, the study from Faria-Neto and coauthors[27] demonstrated that passive immunization with the T15 IgM antibody does not have significant effects on established native aortic atherosclerotic lesions, whereas it reduced vein graft-induced atherosclerotic plaque size in an acute model of atherosclerosis, indicating that anti-OxPL antibodies have therapeutic potential. In the present study, we tested if a novel monoclonal IgM antibody generated through the screening against POVPC/PGPC from the spleens of atherosclerotic *Apoe*$^{-/-}$ mice, could inhibit atherosclerosis development and/or confer beneficial changes in plaque composition in mice with advanced lesions.

MATERIALS AND METHODS

The data that support the findings of this study are available from the corresponding authors upon reasonable request.

Mice

Experiments were conducted according to the guidelines for animal atherosclerosis studies[28] and recommendations about reporting sex in preclinical studies[29] formulated by the American Heart Association.

Animal protocols were approved by the University of Virginia Animal Care and Use Committee. *Apoe*$^{-/-}$ mice (The Jackson Laboratory; #002052), *ROSA26-STOP*^{Flox}*eYFP*$^{+/+}$*;Myh11-CreER*^{T2}*;Apoe*$^{-/-}$(designated as SMC *YFP*$^{+/+}$*ApoE*$^{-/-}$)[9,30,31], secretory *IgM*$^{-/-}$ (*sIgM*$^{-/-}$) mice were kindly provided by Dr. Peter Lobo (University of Virginia) and crossed to *ApoE*$^{-/-}$ mice. We achieved activation of Cre-recombinase in SMC *YFP*$^{+/+}$*ApoE*$^{-/-}$ mice through ten intraperitoneal injections of tamoxifen (Sigma-Aldrich, T-5648) (1 mg in 100 μL peanut oil [Sigma-Aldrich]) over a 10-day period starting at 5–6 weeks of age. All experimental and control mice were treated with tamoxifen in an identical manner. The Myh11-CreERT2 recombinase coding region is inserted within the Y-chromosome, as such only male mice were used for experiments.

Experimental mice were fed a high-fat (Western type) diet containing 21% milk fat and 0.15% cholesterol (Harlan Teklad; TD.88137) starting at 6–8 weeks of age. Irradiated mouse standard laboratory diet was purchased through Harlan (TD.7012). All mice were euthanized after a 4-hour fast, and blood plasma was collected. Peritoneal lavage was collected from mice that received POVPC/PGPC, 25 μg of each, via peritoneal injection six hours in prior sacrifice. Brachiocephalic arteries from mice were harvested, fixed in 4% paraformaldehyde and paraffin or frozen-OCT embedded. Brachiocephalic arteries were sectioned at 10 μm or 5 μm thickness from the aortic arch to the right subclavian artery. Morphometric and immunohistochemical analyses were performed using 2 – 4 sections per artery. Assays of total plasma cholesterol and triglyceride levels were performed by the University of Virginia Clinical Pathology Laboratory.

Human tissues.

Coronary artery specimens from de-identified human subjects were collected during coronary artery bypass graft. These specimens were processed and fixed in paraformaldehyde, and paraffin-embedded blocks were cut into 5 μm sections. The institutional review board at the University of Virginia approved the use of all autopsy specimens.

Monoclonal antibody production, purification, and sequencing

Natural antibodies were obtained from spleens of two *Apoe*$^{-/-}$ male mice fed a Western diet (Harlan Teklad; TD.88137) for seven months. Mice received one booster inter-spleen injection of POVPC/PGPC (25 μg of each) 24 hours before spleen isolation. Hybridoma cells were produced in the University of Virginia Antibody Engineering and Technology Core using a standard protocol[32,33]. Briefly, spleen cells from the mouse were washed once in Iscove's MDM and mixed with washed Sp2/0-Ag14 myeloma cells[34] at a 5:1 ratio (splenocyte to myeloma). The cells were pelleted and the medium aspirated. Cell fusion was accomplished by the stepwise addition of 50% polyethylene glycol (PEG 4,000, Gibco) over one minute. The PEG was then diluted dropwise with Iscove's MDM. The cells were pelleted and gently washed once in Iscove's MDM containing 15% selected fetal bovine serum, hypoxanthine (H), and thymidine (T). The cells were resuspended in HT medium, transferred to a petri dish and incubated at 37C in a humidified atmosphere of 5% CO_2/95% air for one hour. The cells were resuspended in HT medium and plated into 96-well tissue culture plates (Costar, Cambridge, Mass.) at a density of approximately 2 – 4 x 10^5 cells/well. The cultures were fed 24 hours later with HT medium containing aminopterin (HAT medium) and maintained in this medium for two weeks with periodic feeding. Macroscopic colonies usually appeared within 7 – 10 days following the fusion and supernatants are screened for specific antibody production. Antibody-positive hybrids were cloned twice by limiting dilution, and frozen cell stocks were stored in liquid nitrogen cell banks at each stage of hybridoma selection (parental, primary, and secondary clones). Hybridomas were selected based on the cell culture media to bind to POVPC/PGPC in ELISA. A cockroach antigen IgM kappa antibody-producing hybridoma from the University of Virginia hybridoma collection was used as an isotype negative control. IgMs were isolated using HiTrap™ IgM purification HP columns (GE Healthcare). Protein concentration was measured using *DC*™ Protein Assay (BioRad). Total protein was fractioned by electrophoresis under non-denaturing conditions on a 5% polyacrylamide gel. Gels were stained with Coomassie Brilliant Blue.

Amino acid sequencing of the variable region of 10C12 hybridoma

Antibody cloning and sequencing was performed by Syd Labs. Total RNA was extracted from 10C12 hybridoma cells using QIAGEN's RNeasy Kit. cDNA was synthesized from RNA using the SMARTer™ PCR cDNA kit according to the manufacturer's instructions. The cDNA was then used as the template for Rapid Amplification of cDNA Ends (RACE) using the Clontech SMARTer RACE cDNA Amplification kit. PCR reaction samples were analyzed on an agarose gel to visualize the amplified DNA fragments. The correct antibody variable region DNA fragments should have a size between 500–1000 base pairs. PCR

positive clones were TOPO cloned and amplified, followed by gel electrophoresis and recovery from the agarose gel. The amino acid sequences were determined from the nucleotide sequence using standard software. Ten clones were sequenced. Amino acid sequences predicated from the nucleic acid sequence were numbered and designated CDRs of light, and heavy chain of isolated immunoglobulin genes were defined using VBASE2.

Antibody modeling and Molecular docking

Homology modeling of the three-dimensional (3D) structures of scFv 10C12 and scFv E06 were generated from the amino acid sequences using the Rosetta homologous modeling website and models were visualized with the program PyMoL[35]. To understand the molecular interaction of POVPC with the 10C12 scFv antibody, MolSoft software was used to analyze antigen-antibody docking[36]. The POVPC molecule were obtained from the PubChem compound database. The electrostatic density of 10C12 antibody and the binding pocket was predicated and visualized with the program PyMoL. To predict the most critical binding contacts between the 10C12 antibodies and POVPC, the Internal Coordinate Mechanics software (ICM Pro) was used as previously described[37]. Briefly, based on the reaction type, ICM Pro converted the pre-reaction ligand into a “pseudo-ligand” by non-covalently and covalently attaching the side-chain of the electrophilic warhead to all the stereoisomers produced upon addition. Ligand conformations were sampled through Monte Carlo simulations in a set of grid maps calculated for the pocket. Finally, docking solutions were scored and ranked with a modified version of the full ICM scoring function excluding pairwise interactions among the atoms that are directly neighbor the hydrogen and covalent bond link[38].

Oxidized phospholipid ELISA

POVPC/PGPC ELISA protocol was designed and optimized based on previously described protocols[39,40]. Briefly, POVPC, PGPC (Cayman Chemical) or the mixture of both in 96% ethanol were added to 96 well microtiter plates (Nunc), 10 μg per well. Ethanol was quickly evaporated under N_2 flow. Ethanol was used as a negative control. The wells were incubated with 150 μl of blocking solution, 10 % heat deactivated fetal bovine serum (hdFBS) in 1 % PEG 8,000 (Sigma) in phosphate buffered saline (PBS) at 37°C for 1 hour followed by three washes in 1 % PEG in PBS.

POVPC-BSA was prepared by mixing fatty acid-free BSA, 1 mg/mL, with POVPC in a glass tube to get a final concentration of POVPC as 10 μg/mL. LDL,/OxLDL/PH-BSA ELISA protocol was performed as previously described[27]. Ninety-six-well microtiter plate (Nunc) was plated with 100 μL of LDL (Alfa Aesar, BT903), OxLDL (Alfa Aesar, BT-910), PH-BSA (Biosearch Tech, PC-1011-10), or POVPC-BSA (10 μg/mL each) overnight at 4° C. After three washes in PBS, the plate was blocked with 1% BSA (fatty acid-free) at 37°C for 1 hour followed by another three washes in PBS.

Test sera or IgM antibody were diluted as indicated with 10 % hdFBS in 1 % PEG (POVPC/PGPC ELISA) or 1% BSA and aliquoted 50 μl/well onto ELISA plates and incubated at 37°C for 1 hour.After three washes in 1 % PEG in PBS (POVPC/PGPC ELISA) or PBS, peroxidase-coupled anti-mouse (IgG/IgM) secondary antibody (Amersham, NXA931),

diluted at 1:2,000 with 10 % hdFBS in 1 % PEG (POVPC/PGPC ELISA) or 1% BSA in PBS, was added to wells and incubated at 37°C for 1 hour. After three washes in 1 % PEG in PBS (POVPC/PGPC ELISA) or in PBS, peroxidase was developed by ABTS™ (Sigma) substrate solution at room temperature for 30 minutes. Absorbance was measured at 405 nm using a SpectraMax 190 (Molecular Devices).

Surface Plasmon Resonance

To explore direct biomolecular interaction between IgM and PL's, including POVPC, PGPC, and 1,2-dimyristoyl-*sn*-glycero-3-phosphorylcholine (DMPC) in real-time, SPR was performed using a Biacore 3000 instrument (GE Healthcare, Piscataway, New Jersey), according to the manufacturer's instruction. Purified 10C12 IgM was covalently immobilized on a flow cell of CM5 chip (carboxy-methylated dextran coated) in 10 mM sodium acetate buffer, pH 4.0, employing EDC/NHS amine coupling chemistry at 25°C. The unused reactive dextran surface was then inactivated by injecting 1M Etanolamine, pH 8.5. Similarly, the blank control flow cell was successively activated and inactivated without the protein for background subtraction of any non-specific interactions. For kinetic analysis, increasing concentrations of PLs (0 nM, 200 nM, 500 nM, 2000 nM, 10000 nM, and 25000 nM) in the running buffer HBS-P (10 mM HEPES, 0.15 M NaCl, 0.005% polysorbate 20, pH 7.4) containing 1% DMSO were injected at a flow rate of 30 μL/min for 180 seconds. Following dissociation, the chip surface was regenerated with the running buffer. The SPR sensorgrams were quantified to obtain the affinity constant (KD), using the Biacore 3000 Evaluation Software (GE Healthcare) and the Langmuir 1:1 binding model.

IgM ELISA

Secreted IgM levels in plasma were quantified by ELISA as published before[41]. Briefly, 96 well microtiter plates (Corning) were incubated at 4°C overnight with capture antibody (unlabeled IgM 625ng/ml) diluted in coating buffer (0.1M disodium phosphate pH 9.0). Plates were blocked (PBS containing 0.5% BSA, 0.1% TWEEN-20, and 0.01% NaN_3), incubated with samples, and then treated with IgM detection antibody conjugated to alkaline phosphatase for two hours at room temperature. Detection antibodies and dilutions used: murine IgM-AP (1:4000, Southern Biotech). Plates were then developed with pNPP solution (Southern Biotech) for 30–60 minutes and read at 405 nm using a SpectraMax 190 (Molecular Devices). IgM concentration was determined through a standard curve of purified immunoglobulin (Southern Biotech) using a range of 0.098–200 ng/mL. All dilutions were determined through careful titration, and only values within the range of standard curves with readings at least 3-fold higher than negative controls were used.

Immunohistochemical and morphometric analyses.

We performed Modified Russell-Movat (Movat) staining for morphometric analysis of the brachiocephalic arteries. The areas within the external and internal elastic lamina, lesion, lumen, and media areas were measured directly from the digitized images. PicroSirius red staining was performed for analysis of collagen content by measuring birefringence to plane-polarized light. Immunohistochemistry (IH) was performed with antibodies for LGALS3 (Cedarlane; CL8942AP; 0.1 μg/mL), 10C12 (0.3 mg/mL) or IgM control (0.3 mg/mL). We used appropriate negative controls including isotype match nonimmune antibody,

as well as no 1st antibody and no 2nd antibody controls. Staining for IH was visualized by DAB (Acros Organics). Oil Red O staining was performed on frozen brachiocephalic artery sections using Lipid Stain kit (Abcam, ab150678). Images were acquired with Zeiss Axioskope2 fitted with an AxioCamMR3 camera. Image acquisition was performed with AxioVision40 V4.6.3.0 software (Carl Zeiss Imaging Solution). Settings were fixed at the beginning of both acquisition and analysis steps and then were unchanged. Vessel morphometry and areas of positive immunohistochemical or PircoSirius red staining were quantified using ImagePro Plus 7.0 software (Media Cybernetics, Inc) as previously described[9,30,31]. Sudan IV staining was performed on whole aortas as *en face* preparation as previously described[31].

Aortic smooth muscle cells

Male rat aortic smooth muscle cells were previously described[42]. For experiments, cells were grown to 100% confluence and then switched to serum-free media (SFM) (DMEM/F12 [Gibco], 100 U/mL penicillin/streptomycin [Gibco], 1.6 mM/L L-glutamine [Gibco]). After culturing in SFM for 3 days, passages 5–12 of post-confluent rat aortic SMCs were treated with DMSO-vehicle, 10 μg/mL POVPC (Cayman Chemicals) with or without serum-free cultured media from 10C12 hybridoma cells for 24 hours to induce suppression of SMC marker genes.

RNA isolation, cDNA preparation, and qRT-PCR

Abdominal lavage cells and fat samples were harvested from mice. Total RNA was isolated using Trizol reagent (Invitrogen) according to the manufacturer's protocol. One microgram of RNA was reverse-transcribed with iScript cDNA synthesis kit (BioRad). Real-time RT-PCR was performed on a C1000™ Thermal Cycler CFX96™ (BioRad) using SensiFAST™ SYBR NO-ROX Mix (Bioline) and primers specific for mouse *Ho1, Il1b, Mcp1, B2m* as previously described[4,9]. Expression of the genes was normalized to *B2m*.

Statistics.

Normality of the data was determined via the Kolmogorov-Smirnov test. For comparison of 2 groups of continuous variables with normal distribution, 2-tailed Student's *t* tests (for equal variances) or *t*-test with Welch's correction (for unequal variances) were used. Linear mixed-model ANOVA with Tukey's post hoc test was used for multiple group comparison. Two-group comparisons with non-normal distributions were analyzed using the non-parametric Mann-Whitney test. Fisher's exact test was used for categorical data. $P < 0.05$ was considered significant. Statistical outliers were identified as values beyond 3 standard deviations of the mean level and were excluded from analyses. Sample size (number of mice) was chosen based on our previous studies[9,30,31]. SAS v9.3 with Enterprise Guide v5.1 software (SAS Institute Inc.) and GraphPad Prism were used for all statistical analyses. All *in vitro* experiments were done in triplicate for each experimental group and performed in 3 independent experiments. The number of mice used for each *in vivo* analysis is indicated in the Figure legends. For several groups where animal numbers were small due to technical or methodological reasons, we did not use any statistical tests and considered these data only as a trend.

RESULTS

Development and characterization of the 10C12 antibody

Using a previously published anti-OxPL monoclonal antibody production strategy[16], we generated a panel of B-cell hybridomas from spleens of *Apoe*$^{-/-}$ mice fed a high-fat Western diet for seven months that exhibit specificity to POVPC/PGPC mixture (Figure I in the online-only Data Supplement). Of major importance, we found that one hybridoma line, 10C12, produced an IgM kappa antibody that exhibited high titer activity against POVPC/PGPC and inhibited POVPC-induced SMC phenotypic switching *in vitro* (Figure II in the online-only Data Supplement). The 10C12 IgM antibody was purified using HiTrap™ IgM purification HP columns. The purity of 10C12 IgM and specific binding to POVPC/PGPC were confirmed by: 1) SDS-PAGE and staining with Coomassie Brilliant Blue (Figure IIIA in the online-only Data Supplement), and, 2) an OxPL ELISA (Figure IIIB in the online-only Data Supplement). A cockroach antigen IgM kappa antibody with little or no reactivity to OxPLs was used as an isotype control (IgM control) (Figure IIIC in the online-only Data Supplement). To determine if the 10C12 antibody can bind to other PLs, including phosphorylcholine (PC), LDL, oxLDL, and POVPC-BSA, we performed an additional ELISA using the above-mentioned phospholipids as antigens (Figure IIID in the online-only Data Supplement). Results demonstrated that, in contrast to the E06 antibody, 10C12 does not bind to PC-BSA or oxLDL.

To determine if the 10C12 antibody could potentiate an immune response within atherosclerotic lesions *in vivo*, we performed immunostaining on advanced human coronary artery atherosclerotic lesions (Figure 1). 10C12 antibody staining revealed positively stained areas within lesions, whereas the adjacent sections stained with the IgM control antibody, or without first antibody did not show any staining.

To determine whether the 10C12 antibody is genetically similar to the E06/T15 idiotype we sequenced the variable regions of Ig heavy and light chains using the Rapid Amplification of cDNA Ends (RACE) method. The DNA sequence of 10C12 was translated into amino acid sequences using Snap gene software and was aligned using Clustal Omaga software. Figure 2A shows the amino acid sequences for the variable regions of V_H and V_L of the 10C12 antibody, including complimentary determining regions (CDRs). The closest germline sequence of the 10C12 antibody variable region was identified from the IMGT database. Analysis revealed that both the light chain (V_L) and heavy chain (V_H) of 10C12 are 100% mouse germline (Table 1). The light chain variable region of the 10C12 antibody gene belonged to the immunoglobulin mouse kappa, $IGKV_6$ subgroup and contained $IGKJ_5$ gene segments. The heavy chain belonged to the immunoglobulin mouse V_{HII} ($IGHV_2$) subgroup gene family with JH_2 and D_1 segments.

Three-D homology models of scFv were generated based on the amino acid sequence of 10C12 and E06 template using Rosetta software modelling. Structures of heavy and light chains for 10C12 were superposed on the corresponding chain of E06 in the orientation template. The three-dimensional overlapping models of scFv 10C12 and E06 are shown in Figure 2B. The orientation of the CDR loops of the 10C12 antibody that are different from the corresponding loops in the E06 antibody are indicated by arrows. The 10C12 antibody

paratope CDR loops provided a polar electrostatics density (Figure IVA in the online-only Data Supplement). The backbone conformations of the bases of the CDR-H3 loop have a C-terminal kinked class[35,43], a structure that resembles a β bulge in that it disrupts the hydrogen bonding pattern along a β strand and causes the backbone to twist. The results of sequencing and rearrangement with CDRs of the E06/T15 antibody clearly indicate that the 10C12 antibody is genetically and structurally distinct from the classic T15 antibody (Figure 2A and B).

Given that POVPC/PGPC ELISA response to the 10C12 antibody was relatively weak as compared to classical protein-based ELISA, we performed a Surface Plasmon Resonance (SPR) assay to investigate the specificity of the 10C12 antibody. The 10C12 IgM antibody was immobilized on the spotted SPR biochip. To obtain kinetic parameters, different concentrations (200 nM – 25 μM) of PLs, including POVPC, PGPC, and control non-oxidized phospholipid, 1,2-dimyristoyl-sn-glycero-3- phosphorylcholine (DMPC), were injected into the biochip, and the SPR signals were analyzed after subtraction of the background noise. Sensorgams for the binding of 10C12 to POVPC, PGPC, and DMPC are presented in Figure 3. As expected, the profile of the SPR signal for POVPC demonstrated a sharp increase in SPR signal during the association phase, and gradual slow decrease during the dissociation phase, indicating a specific interaction with the binding constant K_D = 2.6 μM (Figure 3). In contrast, interaction experiments on both DMPC and PGPC resulted in the atypical curves with very low (< 0.03) maximal feasible signal (R_{max}), indicating that these interactions highly likely are non-specific and preventing us from getting correct kinetic parameters. Interestingly, the atypical profile of the SPR signal for PGPC showed a relatively sharp increase in the SPR signal during association phase with fast immediate decrease, suggesting that PGPC may interact with 10C12, but this interaction is unstable. Taken together, our SPR data suggest that 10C12 recognizes oxidized rather than non-oxidized phospholipids and that the aldehyde group in POVPC has high affinity and further oxidation to the acid leads to a sharp reduction in affinity.

To predict the most critical binding contacts between the 10C12 antibodies and POVPC we used the Internal Coordinate Mechanics (ICM) method[44]. Molecular docking analysis predicted that the V_H domain of CDR3 and V_L domain of CDR3 provided the main contact to POVPC as shown in Figure IVB (in the online-only Data Supplement). As shown in Figure IVC (in the online-only Data Supplement), the key residues of the heavy chain, H^{S100}, H^{S100a}, H^{H100c}, and light chain L^{Y91} hydroxyl and amine groups, provide non-covalent bonds with the polar oxygens of POVPC. In addition, the aromatic ring π-electron and amine of the heavy chain tryptophan residue, H^{W100b}, forms the non-covalent interaction with the oxygen of POVPC (Figure IVC in the online-only Data Supplement). Importantly, the aldehyde group has additional binding capacity to stabilize/enforce the binding through the polar groups of serine (H^{S100a}) and histidine (H^{H100c}) hydroxyl and amine groups.

The 10C12 antibody can prevent early inflammatory responses in Western diet-fed Apoe$^{-/-}$ mice in vivo

Apoe$^{-/-}$ mice have previously been reported to have the early accumulation of macrophages within atheroprone areas within four weeks of initiation of high-fat Western diet feeding[45]. To examine if 10C12 IgM treatment can prevent the early development of atherosclerosis, we injected five-week-old *Apoe*$^{-/-}$ mice intraperitoneally (IP) with 150 μg 10C12 IgM, control IgM (IgMc) or saline (Sham) twice a week for five weeks. Over the last four weeks, mice were switched to either a Western diet or continued on a standard laboratory diet for the Sham control group (Figure 4A). Mice treated with 10C12, IgM control or Sham did not show any difference in cholesterol or triglycerides levels in response to Western diet feeding but demonstrated a ~3 fold increase in cholesterol as compared to a low fat standard laboratory diet-fed mice treated with Sham-control (Figure VC in the online-only Data Supplement). Of major interest, we found a significant decrease in the accumulation of cells positive for LGALS3, a traditional marker of macrophages but also expressed in a subset of SMC-derived macrophage-like lesion cells[30], after 10C12 IgM treatment as compared to Sham treatment (Figure 4B and C, Figure VI in the online-only Data Supplement). Moreover, we demonstrated that 10C12 antibody injections in *Apoe*$^{-/-}$ mice fed a Western diet for four weeks resulted in high circulating titers of antibodies to POVPC/PGPC as measured by ELISA (Figure VB in the online-only Data Supplement).

To examine whether the 10C12 antibody had a systemic neutralizing effect, we performed IP injections of POVPC/PGPC, 25 μg of each, and six hours later (Figure 4A) analyzed an OxPL-induced inflammatory response in abdominal lavage cells as previously described[46]. We observed a significant decrease in OxPL-induced *Ho1* gene expression in mice that had received five weeks of the 10C12 antibody treatment (Figure 4D). 10C12 also appeared to modestly decrease expression of *Il1b* or *Mcp1* within POVPC/PGPC-stimulated abdominal lavage cells as compared to IgM control treated animals, but these just failed to achieve statistical significance with *P* values of 0.08 and 0.10 respectively (Figure VD and E in the online-only Data Supplement).

Taken together these results indicate that the 10C12 antibody can prevent early macrophage accumulation and inflammatory responses in *Apoe*$^{-/-}$ mice *in vivo*.

The 10C12 antibody does not alter advanced plaque pathogenesis in Apoe$^{-/-}$ mice on a long term high-fat diet

We next sought to determine whether the 10C12 antibody could decrease and/or reverse the development of atherosclerosis in late stages of the disease as this would mimic likely clinical paradigms. For this experiment we utilized the SMC-specific conditional eYFP lineage tracing *Apoe*$^{-/-}$ mice fed a Western diet previously described by our lab (designated as SMC *YFP*$^{+/+}$*ApoE*$^{-/-}$)[9,30,31]. This provides us the ability to determine if the 10C12 antibody treatment promotes phenotypic transitions of SMC beneficial in promoting plaque stability including contributing to myofibroblast-like ACTA2^{+} fibrous cap cells rather than formation of SMC-derived pro-inflammatory macrophage-like cells and foam cells. SMC *YFP*$^{+/+}$*ApoE*$^{-/-}$ mice were fed a Western diet for eighteen weeks to induce the formation of advanced atherosclerotic lesions. After eighteen weeks of a Western diet, mice were then

treated by weekly IP injections with 150 μg 10C12, IgM control or Sham for 8 weeks, and Western diet feeding was continued throughout the duration of the experiment (Figure VIIA in the online-only Data Supplement). Mice injected with 10C12, IgM control or Sham exhibited no significant differences in total cholesterol, HDL-cholesterol, triglycerides, body weights (Figure VIIB in the online-only Data Supplement) or inflammatory marker mRNA levels in the abdominal fat as assessed by qRT-PCR (Figure VIIC in the online-only Data Supplement). Mice treated with the 10C12 antibody demonstrated a significant decrease in LDL/HDL or total cholesterol/HDL ratios as compared to the IgM control-treated group (Figure VIIB in the online-only Data Supplement). In contrast to the athero-protective effect in the four-week Western diet experiment, 10C12 antibody treatment in mice with advanced stage atherosclerotic lesions had no effect on lesion size or lumen and external elastic lamina (EEL) area (Figure VIIIA–C in the online-only Data Supplement) as compared to IgM control- or Sham-treated mice. There were also no differences in indices of plaque stability, including the number of smooth muscle (YFP^+) cells (Figure VIIID in the online-only Data Supplement), the total number of $LGALS3^+$ cells or SMC-derived $YFP^+LGALS3^+$ macrophage-like cells (data not shown) within a 30 μm fibrous cap area, the total collagen content and the collagen fiber maturation within the lesion based on PicroSirius Red staining followed by polarized microscopy (Figure VIIIE and F in the online-only Data Supplement), and intraplaque hemorrhage based on the red blood cell marker TER119 staining (data not shown).

Given that the 10C12 antibody treatment had a positive effect on LDL/HDL and total cholesterol/HDL ratios in *Apoe*$^{-/-}$ mice fed a long-term Western diet, but no discernable changes in lesion size or composition, we increased the number of IgM injections to two injections per week to test if a higher titer of 10C12 can inhibit further progression of atherosclerosis and/or increase indices of plaque stability. However, this experiment could not be completed due to a high mortality rate in both 10C12 and IgM control treatment groups.

The 10C12 antibody decreases atherosclerosis development in sIgM$^{-/-}$Apoe$^{-/-}$ mice fed a low fat diet

There are several possible explanations for the failure of the 10C12 antibody to positively impact multiple parameters of lesion pathogenesis in mice with advanced lesions. A likely explanation is that this class of antibody may not be capable of conferring benefit in the context of the extreme hyperlipidemic state and high natural IgM antibody titers characteristic of the *Apoe*$^{-/-}$ Western diet model. To test both of these possibilities, we utilized previously described[21,41] mice deficient in secretory IgM to avoid the high IgM background present in *Apoe*$^{-/-}$ mice fed a high-fat diet. *sIgM*$^{-/-}$ mice were crossed to the *Apoe*$^{-/-}$ background and fed either a low-fat standard laboratory diet or Western diet. There were no detectable levels of IgM in *sIgM*$^{-/-}$*Apoe*$^{-/-}$ mice, confirming a high efficiency of IgM deficiency. Consistent with previous studies, Western diet feeding induced a significant increase in plasma IgM in *Apoe*$^{-/-}$ mice (Figure 5A). A previous study reported that *sIgM*$^{-/-}$*Ldlr*$^{-/-}$ mice demonstrated accelerated atherosclerosis as compared to *Ldlr*$^{-/-}$ mice on both a low-fat and high-fat diet[21]. Consistent with our hypothesis that the 10C12 antibody treatment failed due to the high cholesterol levels in Western diet-fed *Apoe*$^{-/-}$ mice, we

found that *sIgM*$^{-/-}$*Apoe*$^{-/-}$ mice fed a Western diet for twelve (Figure 5B **and** C) or eight (unpublished observations) weeks show no significant difference in atherosclerotic lesion development as compared to *Apoe*$^{-/-}$ mice. However, these *sIgM*$^{-/-}$*Apoe*$^{-/-}$ mice fed a standard laboratory diet for forty weeks showed an increase in en face lipid accumulation as compared to control mice fed a Western diet (Figure 5D **and** E). Importantly, *Apoe*$^{-/-}$ and *sIgM*$^{-/-}$*Apoe*$^{-/-}$ mice fed a standard laboratory diet demonstrated ~2-fold lower total cholesterol and LDL content as compared to mice fed a Western diet for 18 weeks (Figure 5F versus Figure VIIB in the online-only Data Supplement) There were no significant differences in total cholesterol, LDL-cholesterol or HDL-cholesterol levels between standard laboratory diet fed *sIgM*$^{-/-}$*Apoe*$^{-/-}$ and *Apoe*$^{-/-}$ groups, but a significant increase in triglycerides (Figure 5F).

Therefore, for the intervention study, 32-week-old *sIgM*$^{-/-}$*Apoe*$^{-/-}$ mice were IP-injected with 150 μg 10C12 IgM or control IgM twice a week for eight weeks (Figure 6A). The 10C12-treated mice demonstrated a modest significant decrease in cholesterol levels and a near significant decrease in LDL levels ($P = 0.09$) (Figure 6B). There were no significant differences in HDL, triglycerides or body weights between 10C12- and IgM control-treated animals (Figure 6B). Blood plasma IgM titers measured by ELISA demonstrated equal IgM levels for both 10C12 and IgM control animal groups (Figure 6C), but no difference in IgG levels (Figure IX in the online-only Data Supplement) Of major significance, whole aorta *en face* Sudan IV lesion staining analyses revealed a 40% decrease in atherosclerotic plaque area after 10C12 IgM treatment (Figure 6D and E). In addition, Oil Red O staining of the brachiocephalic artery cross-sections showed a decrease in lipid accumulation within the tunica media along the artery (Figure 6F) in 10C12 IgM treated animals as compared to IgM control treated animals. To test if there was a correlation between animals with elevated cholesterol and increased Sudan IV positive plaque areas, we performed the Pearson's correlation test. There was no statistically significant correlation between cholesterol and lipid accumulation [$r = 0.16$, P(two-tailed) = 0.6], indicating that the 7% difference in cholesterol levels between treatment groups was not a primary driver of the 10C12 effect on lipid accumulation.

DISCUSSION

There is overwhelming evidence that OxPL such as PAPC and its derivatives are prevalent within atherosclerotic lesions and induce marked proinflammatory responses in vascular SMC, endothelial cells, and immune cells *in vitro*. There is also extensive correlative evidence suggesting that auto IgM antibodies to the phosphorylcholine head groups on the OxPL are atheroprotective including observations that patients with low OxPL IgM antibody titers have an increased incidence of CAD[47,48]. However, despite numerous claims that these OxPL are critical in the pathogenesis of atherosclerosis, direct evidence for this was lacking until recent elegant work by Witztum and colleagues showing that transgenic *Ldlr*$^{-/-}$ mice expressing a single chain variable fragment of these OxPL antibodies were protected from the development of vascular inflammation and atherosclerosis upon Western diet feeding[26]. These studies are critical in that they validate decades of intensive investigation of the potential role of OxPLs in the pathogenesis of atherosclerosis and suggest that therapies inactivating OxPL may be beneficial for treating atherosclerosis. However, these studies

involved prevention of atherosclerosis, not intervention once atherosclerosis is established which is the likely scenario for treating patients with the advanced clinical disease, and of course, transgene approaches are not feasible in humans. The studies presented herein are the first to provide direct evidence that administration of auto IgM antibodies, 10C12, generated through the screening against POVPC/PGPC can inhibit atherosclerosis development *in vivo* in a mouse model of atherosclerosis. However, several caveats in our observations are likely to have important implications for efforts to develop possible OxPL antibody-based therapies for treating humans with advanced atherosclerosis. First, we were able to show sustained benefits only when the 10C12 antibody was administered to *Apoe*$^{-/-}$ mice that were unable to mount their own endogenous OxPL IgM antibody response and were fed a standard low-fat laboratory diet rather than a high-fat Western diet. Second, consistent with a previous report from Faria-Neto and co-authors[27], our antibody had no demonstrable effect on lesion pathogenesis when administered to Western diet-fed *Apoe*$^{-/-}$ mice that already had established atherosclerosis. Third, we observed no difference in atherosclerosis development in *sIgM*$^{-/-}$*Apoe*$^{-/-}$ versus IgM wild type *Apoe*$^{-/-}$ mice on a Western diet.

Taken together these results suggest that: 1) mice, and probably humans, are capable of mounting a robust immune response to OxPL such that addition of exogenous OxPL antibodies may have a negligible effect; and 2) that severe hyperlipidemia can overwhelm the protective effects of these auto IgM antibodies. Extensive further studies will be required to test these possibilities. However, it is interesting to speculate that OxPL autoimmune Ab-based therapies might have increased efficacy in conjunction with primary therapies that effectively reduce lipids and the concentration of OxPL within lesions, as well as in patients harboring genetic mutations that impair their OxPL antibody response. For example, we have previously identified an Id3 mutation linked to reduced B-cell-mediated atheroprotection in both mice and humans[49].

Although, the 10C12 antibody did not have a similar structure to the previously described panel of E0/T15 idiotype antibodies to epitopes of OxLDL from *Apoe*$^{-/-}$ mice, including the anti-POVPC E06 antibody, the heavy chain CDR3 (HCDR3) amino acid sequence of two hybridomas have high homology. The HCDR3 loop in antibodies is often the most important loop for antigen binding. The variable heavy chain of E06 CDR3 region is derived from V_{HVII} (IGHV7), JH1, and D1 segments, and 10C12 CDR3 is derived from V_{HII} (IGHV2), JH2, and D1 segments of different germ lines. The 10C12 hybridoma has a longer heavy chain CDR3 (HCDR3), one amino acid insertion, as compared to E06 HCDR3. It is notable that so many different rearranged V_H genes of HCDR3, a dataset that was generated by sequencing the naïve B cell repertoire that were derived from 19 germline genes, were found to contain the same HCDR3[50]. This result indicates that the generation identical HCDR3s from different germline genes is either biological in nature, or a result of the molecular biological influences. The structure of HCDR3, despite having the same amino acid sequence, exhibits the largest conformational diversity. One assumption is that the HCDR3 conformations are influenced by both their amino acid sequence and their structural environment determined by the heavy and light chain pairing. It is perhaps not surprising given a recent report in which structural analysis of the same HCDR3 sequence placed within the context of different V_H and V_L genes shows significant conformational

diversity[51]. Here, the 10C12 antibody heavy chain is pairing a different light chain sequence as compared to E06, suggesting that the paratope conformation of the 10C12 antibody is modified not only by its HCDRs sequences but also by its V_H and V_L pairing.

Using massively parallel sequencing of the HCDR3 regions of murine B-1 cell subsets, the Witztum group recently found that the classic E06/T15 idiotype occurred only infrequently[52]. Notably, they identified another HCDR3 sequence (CMRYGNYWYFVW) that was much more common and bound phosphorylcholine and OxPLs, suggesting that other common HCDR3 regions outside of the classical E06/T15 bind oxidation selection epitopes and may provide protection from atherosclerosis. In addition, the splenic B-1a cell repertoire had more N additions and unique sequences than those in the peritoneal cavity, suggesting that these antibodies may result from post-natal selection of B1a cells in response to oxidation selection epitopes and apoptotic cells. Another recent report demonstrated a high frequency of somatic mutations in the V(D)J regions encoding specific CDR3 peptides in B-1a cells of aged mice, suggesting that those mutations, and the resultant repertoire of natural antibodies are age dependent[53]. While, like the Witztum's group, our studies were performed in B6 mice, unlike their studies, our mice were older and had hyperlipidemia. The HCDR3 of 10C12 (ARNGYYGSSWHYFDY) is distinct from both that of E06/T15 (DYYGSSYWYFDV) and the OxPL-binding antibody (CMRYGNYWYFVW) they identified, suggesting that age and hyperlipidemia may impact on the B-1a-derived antibody repertoire.

To further investigate structural and antigen binding characteristics of the 10C12 antibodies, we performed a series of computer modeling evaluation. To be able to modulate binding to a large spectrum of potential antigens the H3 is known to have very high structural variability. It has been previously suggested that the source of its structural variability is increased flexibility because of its longer length and lack of stabilizing bonds. Further, HCDR3 loop has a higher propensity for Tyrosine (Tyr), Glycine (Gly), Aspartic Acid (Asp), and Phenylalanine (Phe). Correspondingly, CDR H2 has a higher propensity for Serine (Ser) and Gly than the general amino acids set[54]. The high abundance of Tyr, Ser, and Gly in natural antibody germ-line sequences reflects the intrinsic capacity of these residues to arbitrate antigen recognition[55]. The physicochemical properties of Tyr make it the amino acid that is most effective for mediating molecular recognition in terms of affinity and specificity[56]. In this study, antibody molecular modeling and amino acid sequence analyses indicated that the 10C12 CDRH3 loop tends to be longer and has a higher propensity to have a high abundance of Tyr, Ser, and Gly residues. Similarly, the 10C12 HCDR2 loop also has a higher propensity to have a high abundance of Ser and Gly residues. The HCDR3 of 10C12 has a crucial role in facilitating the recognition of antigens; as shown in Figure IV (in the online-only Data Supplement), by extending and changing its conformation upon antigen binding.

Intriguingly, using the SPR technique that allows measuring the kinetics of binding for two molecules, we found that only POVPC, but not PGPC, binds specifically to 10C12. Given that the only difference between POVPC and PGPC is an aldehyde group in POVPC versus carboxyl group in PGPC, we can conclude that the aldehyde group is crucial for binding to 10C12. Of major importance, the ICM molecular docking analysis revealed that the

aldehyde group has additional binding capacity to stabilize/enforce the connection through the binding to the CDR3 heavy chain residue, H^{S100a} and H^{H100c} (Figure IVC in the online-only Data Supplement). Interestingly, previous studies proposed that POVPC aldehyde groups form aldol condensation adducts and these adducts are highly antigenic to the E06 antibody, whereas the freshly isolated POVPC is not antigenic when immediately tested for E06 recognition[22]. Indeed, the authors concluded that the key epitope for E06 recognition is the phosphorylcholine core[22]. It is thus possible there may be a similar effect with the 10C12 antibody. However, we neither found any binding with the non-oxidized phosphorylcholine phospholipid DMPC, nor observed any ELISA signal with PC-BSA or OxLDL. Therefore, we conclude that the aldehyde group is crucial for the binding with 10C12.

Although in this manuscript we refer to the 10C12 as the anti-POVPC antibody based on the screening strategy we used to generate it, SPR, and molecular docking prediction results, there are still many uncertainties regarding 10C12 specificity and reactivity. Our results clearly demonstrate that reactivity of the 10C12 antibody along with its idiotype and structure differ from the E06/T15 antibody, but they do not provide clear evidence for its specificity for other OxPLs. Future studies will be required to validate the results of computer modeling, including mutation of CDR sequences and extensive screening of different oxidized as well as non-oxidized phospholipids for 10C12's ability to bind to them and neutralize their activity.

In conclusion, we have isolated a novel autoantibody from the spleens of atherosclerotic *Apoe*$^{-/-}$ mice fed a long term Western diet with potential neutralizing activity to oxidized phospholipids. We show that this antibody has an ability to attenuate the development of atherosclerosis, suggesting that anti-OxPL antibody treatment has potential as an anti-atherosclerosis therapeutic. However, a single OxPL IgM antibody appears to have limited capability of conferring benefit beyond what is conferred by the host innate immune response to OxPL epitopes, and further studies are needed to find a way to enhance the efficacy of this therapeutic approach, and/or to identify patients who might show greater benefit because their innate immune response is impaired.

Supplementary Material

Refer to Web version on PubMed Central for supplementary material.

ACKNOWLEDGMENTS

The authors would like to thank R. Tripathi, M. Bevard, A. Washington, and C. Pletz for technical assistance; E. Podrez and V. Serbulea for discussion. V. Flores-Malavet for help with image analysis; S. Adams, D. Adams, Dr. W. Sutherland from the Lymphocyte Culture Center, University of Virginia for help with generating B-cell hybridomas; and, E. Poptic from the Hybridoma Core, Lerner Research Institute, Cleveland Clinic for help with OxPL ELISA design. We would like to thank Dr. J. Witztum from the University of California, San-Diego for providing the E06 antibody, as well as for discussion and advice. We would like to thank Y. Neuendorf for designing the cartoon in SFigure IB.

O.A.C. conducted most of the experiments, performed data analysis, generated most of the experimental mice and was the primary writer of the manuscript. P.S. provided sIgM$^{-/-}$*Apoe*$^{-/-}$ mice, performed IgM and IgG ELISA and *en face* Sudan IV staining and analysis. E.S.G. assisted with IgM purification protocol optimization and contributed to animal studies. R.M.H. performed image analyses. M.E.M. assisted with POVPC/PGPC ELISA

protocol optimization and IgM purification. M.C and S.B. performed Surface Plasmon Resonance. B.B. assisted with interpretation of 10C12 IgM sequencing results and performed an antibody structure computer modeling. N.L. and C.A.M. provided reagents and advice throughout the project. All authors participated in making final manuscript revisions. G.K.O. supervised the entire project and had a major role in experimental design, data interpretation, and writing the manuscript.

SOURCES OF FUNDING

This work was supported by NIH grants R01 HL132904, R01 HL087867, R01 HL098538, and R01 HL136314 (to G.K.O), R01 HL136098-01, R01 HL107490 (to C.A.M), R01 DK096076, P01 HL120840 (to N.L.), Ivy Foundation Grant (to O.A.C. and G.K.O.). O.A.C. was supported by American Heart Association Research Innovation Grant (17IRG33370017), P.S. was supported by American Heart Association Career Development Grant (18CDA34110392).

Nonstandard Abbreviations and Acronyms

OxPL	Oxidized Phospholipids
PAPC	1-palmitoyl-2-arachidonoyl-*sn*-glycero-3-phosphorylcholine
PGPC	1-palmitoyl-2-glutaroyl-*sn*-glycero-3-phosphorylcholine
POVPC	1-palmitoyl-2-(5-oxovaleroyl)-*sn*-glycero-3-phosphorylcholine
DMPC	1,2-dimyristoyl-*sn*-glycero-3-phosphorylcholine
PC	phosphorylcholine
SPR	Surface Plasmon Resonance
SMC	Smooth Muscle Cell
LDL	Low Density Lipoprotein
OxLDL	Oxidized Low Density Lipoprotein
CDR	Complimentary Determining Region
IP	Intraperitoneally
PEG	Polyethylene Glycol

REFERENCES

1. Berliner JA, Leitinger N, Tsimikas S. The role of oxidized phospholipids in atherosclerosis J Lipid Res. 2009; 50(Supplement):S207–S212. doi:10.1194/jlr.R800074-JLR200 [PubMed: 19059906]
2. Lee S, Birukov KG, Romanoski CE, Springstead JR, Lusis AJ, Berliner JA. Role of Phospholipid Oxidation Products in Atherosclerosis. Circ Res. 2012; 111:778–799. doi:10.1161/CIRCRESAHA.111.256859 [PubMed: 22935534]
3. Freigang S. The regulation of inflammation by oxidized phospholipids. Eur J Immunol. 2016; 46:1818–1825. doi:10.1002/eji.201545676 [PubMed: 27312261]
4. Kadl A, Meher AK, Sharma PR, et al. Identification of a novel macrophage phenotype that develops in response to atherogenic phospholipids via Nrf2. Circ Res. 2010; 107:737–746. doi:10.1161/CIRCRESAHA.109.215715 [PubMed: 20651288]
5. Leitinger N. Oxidized phospholipids as modulators of inflammation in atherosclerosis. Curr Opin Lipidol. 2003; 14:421–430. doi:10.1097/01.mol.0000092616.86399.dc [PubMed: 14501580]

6. Yoshida T, Gan Q, Owens GK. Kruppel-like factor 4, Elk-1, and histone deacetylases cooperatively suppress smooth muscle cell differentiation markers in response to oxidized phospholipids. Am J Physiol Cell Physiol. 2008; 295:C1175–82. doi:10.1152/ajpcell.00288.2008 [PubMed: 18768922]
7. Pidkovka NA, Cherepanova OA, Yoshida T, et al. Oxidized phospholipids induce phenotypic switching of vascular smooth muscle cells in vivo and in vitro. Circ Res. 2007; 101:792–801. doi: 10.1161/CIRCRESAHA.107.152736 [PubMed: 17704209]
8. Cherepanova OA, Pidkovka NA, Sarmento OF, et al. Oxidized phospholipids induce type VIII collagen expression and vascular smooth muscle cell migration. Circ Res. 2009; 104:609–618. doi: 10.1161/CIRCRESAHA.108.186064 [PubMed: 19168440]
9. Cherepanova OA, Gomez D, Shankman LS, et al. Activation of the pluripotency factor OCT4 in smooth muscle cells is atheroprotective. Nat Med. 2016; 22:657–665. doi:10.1038/nm.4109 [PubMed: 27183216]
10. Nicolo D, Monestier M. Antiphospholipid antibodies and atherosclerosis. Clin Immunol. 2004; 112:183–189. doi:10.1016/j.clim.2004.02.016 [PubMed: 15240162]
11. Tacke F, Ginhoux F, Jakubzick C, van Rooijen N, Merad M, Randolph GJ. Immature monocytes acquire antigens from other cells in the bone marrow and present them to T cells after maturing in the periphery. J Exp Med. 2006; 203:583–597. doi:10.1084/jem.20052119 [PubMed: 16492803]
12. Tsimikas S, Kiechl S, Willeit J, et al. Oxidized Phospholipids Predict the Presence and Progression of Carotid and Femoral Atherosclerosis and Symptomatic Cardiovascular Disease. J Am Coll Cardiol. 2006; 47:2219–2228. doi:10.1016/j.jacc.2006.03.001 [PubMed: 16750687]
13. Binder CJ, Silverman GJ. Natural antibodies and the autoimmunity of atherosclerosis. Springer Semin Immunopathol. 2005; 26:385–404. doi:10.1007/s00281-004-0185-z [PubMed: 15609021]
14. Ylä-Herttuala S, Palinski W, Butler SW, Picard S, Steinberg D, Witztum JL. Rabbit and human atherosclerotic lesions contain IgG that recognizes epitopes of oxidized LDL. Arterioscler Thromb Vasc Biol. 1994; 14:32–40. 10.1161/01.ATV.14.1.32
15. Hörkkö S, Binder CJ, Shaw PX, et al. Immunological responses to oxidized LDL. Free Radic Biol Med. 2000; 28:1771–1779. doi:10.1016/S0891-5849(00)00333-6 [PubMed: 10946219]
16. Palinski W, Hörkkö S, Miller E, et al. Cloning of monoclonal autoantibodies to epitopes of oxidized lipoproteins from apolipoprotein E-deficient mice. Demonstration of epitopes of oxidized low density lipoprotein in human plasma. J Clin Invest. 1996; 98:800–814. doi:10.1172/JCI118853 [PubMed: 8698873]
17. Palinski W, Tangirala RK, Miller E, Young SG, Witztum JL. Increased autoantibody titers against epitopes of oxidized LDL in LDL receptor-deficient mice with increased atherosclerosis. Arterioscler Thromb Vasc Biol. 1995; 15:1569–1576. doi:10.1161/01.ATV.15.10.1569 [PubMed: 7583529]
18. Shaw PX, Hörkkö S, Chang MK, et al. Natural antibodies with the T15 idiotype may act in atherosclerosis, apoptotic clearance, and protective immunity. J Clin Invest. 2000; 105:1731–1740. doi:10.1172/JCI8472 [PubMed: 10862788]
19. Snapper CM, Shen Y, Khan AQ, et al. Distinct types of T-cell help for the induction of a humoral immune response to Streptococcus pneumoniae. Trends Immunol. 2001; 22:308–311. doi:10.1016/S1471-4906(01)01926-3. [PubMed: 11377289]
20. Binder CJ, Hörkkö S, Dewan A, et al. Pneumococcal vaccination decreases atherosclerotic lesion formation: molecular mimicry between Streptococcus pneumoniae and oxidized LDL. Nat Med. 2003; 9:736–743. doi:10.1038/nm876 [PubMed: 12740573]
21. Lewis MJ, Malik TH, Ehrenstein MR, Boyle JJ, Botto M, Haskard DO. Immunoglobulin M is required for protection against atherosclerosis in low-density lipoprotein receptor-deficient mice. Circulation. 2009; 120:417–426. doi:10.1161/CIRCULATIONAHA.109.868158 [PubMed: 19620499]
22. Friedman P, Horkko S, Steinberg D, Witztum JL, Dennis EA. Correlation of antiphospholipid antibody recognition with the structure of synthetic oxidized phospholipids. Importance of Schiff base formation and aldol condensation. J Biol Chem. 2002; 277:7010–7020. doi:10.1074/jbc.M108860200 [PubMed: 11744722]

23. Hörkkö S, Bird DA, Miller E, et al. Monoclonal autoantibodies specific for oxidized phospholipids or oxidized phospholipid-protein adducts inhibit macrophage uptake of oxidized low-density lipoproteins. J Clin Invest. 1999; 103:117–128. doi:10.1172/JCI4533 [PubMed: 9884341]
24. Matt U, Sharif O, Martins R, et al. WAVE1 mediates suppression of phagocytosis by phospholipid-derived DAMPs. J Clin Invest. 2013; 123:3014–3024. doi:10.1172/JCI60681 [PubMed: 23934128]
25. Chang MK, Bergmark C, Laurila A, et al. Monoclonal antibodies against oxidized low-density lipoprotein bind to apoptotic cells and inhibit their phagocytosis by elicited macrophages: evidence that oxidation-specific epitopes mediate macrophage recognition. Proc Natl Acad Sci U S A. 1999; 96:6353–6358. doi:10.1073/pnas.96.11.6353 [PubMed: 10339591]
26. Que X, Hung M-Y, Yeang C, et al. Oxidized phospholipids are proinflammatory and proatherogenic in hypercholesterolaemic mice. Nature. 2018; 558:301–306. doi:10.1038/s41586-018-0198-8 [PubMed: 29875409]
27. Faria-Neto JR, Chyu K-Y, Li X, et al. Passive immunization with monoclonal IgM antibodies against phosphorylcholine reduces accelerated vein graft atherosclerosis in apolipoprotein E-null mice. Atherosclerosis. 2006; 189:83–90. doi:10.1016/j.atherosclerosis.2005.11.033 [PubMed: 16386745]
28. Daugherty A, Tall AR, Daemen MJAP, et al. Recommendation on Design, Execution, and Reporting of Animal Atherosclerosis Studies: A Scientific Statement From the American Heart Association. Arterioscler Thromb Vasc Biol. 2017; 37:e131–e157. doi:10.1161/ATV.0000000000000062 [PubMed: 28729366]
29. Robinet P, Milewicz DM, Cassis LA, Leeper NJ, Lu HS, Smith JD. Consideration of Sex Differences in Design and Reporting of Experimental Arterial Pathology Studies-Statement From ATVB Council. Arterioscler Thromb Vasc Biol. 2018; 38:292–303. doi:10.1161/ATVBAHA.117.309524 [PubMed: 29301789]
30. Shankman LS, Gomez D, Cherepanova OA, et al. KLF4-dependent phenotypic modulation of smooth muscle cells has a key role in atherosclerotic plaque pathogenesis. Nat Med. 2015; 21:628–637. doi:10.1038/nm.3866 [PubMed: 25985364]
31. Durgin BG, Cherepanova OA, Gomez D, et al. Smooth muscle cell-specific deletion of col15α1 unexpectedly leads to impaired development of advanced atherosclerotic lesions. Am J Physiol - Hear Circ Physiol. 2017; 312:H943–H958. doi:10.1152/ajpheart.00029.2017
32. Chapman MD, Sutherland WM, Platts-Mills TA. Recognition of two Dermatophagoides pteronyssinus-specific epitopes on antigen P1 by using monoclonal antibodies: binding to each epitope can be inhibited by serum from dust mite-allergic patients. J Immunol. 1984; 133:2488–2495. [PubMed: 6207232]
33. Chang JH, Sutherland WM, Parsons SJ. Monoclonal antibodies to oncoproteins. Methods Enzymol. 1995; 254:430–445. doi:10.1016/0076-6879(95)54029-6 [PubMed: 8531704]
34. Shulman M, Wilde CD, Köhler G. A better cell line for making hybridomas secreting specific antibodies. Nature. 1978; 276:269–270. doi:10.1038/276269a0 [PubMed: 714156]
35. Weitzner BD, Jeliazkov JR, Lyskov S, et al. Modeling and docking of antibody structures with Rosetta. Nat Protoc. 2017; 12:401–416. doi:10.1038/nprot.2016.180 [PubMed: 28125104]
36. Totrov M. Estimated secondary structure propensities within V1/V2 region of HIV gp120 are an important global antibody neutralization sensitivity determinant. PLoS One. 2014; 9:e94002. doi:10.1371/journal.pone.0094002 [PubMed: 24705879]
37. Raush E, Totrov M, Marsden BD, Abagyan R. A New Method for Publishing Three-Dimensional Content. Gay N, ed. PLoS One. 2009; 4:e7394. doi:10.1371/journal.pone.0007394 [PubMed: 19841676]
38. Lam PC-H, Abagyan R, Totrov M. Ligand-biased ensemble receptor docking (LigBEnD): a hybrid ligand/receptor structure-based approach. J Comput Aided Mol Des. 2018; 32:187–198. doi:10.1007/s10822-017-0058-x [PubMed: 28887659]
39. Rolla R, Vidali M, Serino R, Pergolini P, Albano E, Bellomo G. Antibodies against oxidized phospholipids in laboratory tests exploring lupus anti-coagulant activity. Clin Exp Immunol. 2007; 149:63–69. doi:10.1111/j.1365-2249.2007.03404.x [PubMed: 17488295]

40. Kilpatrick DC. Factors affecting cardiolipin antibody assays: modification with polyethylene glycol compound. Br J Haematol. 1998; 100:52–57. 10.1046/j.1365-2141.1998.00532.x [PubMed: 9450790]
41. Harmon DB, Srikakulapu P, Kaplan JL, et al. Protective Role for B-1b B Cells and IgM in Obesity-Associated Inflammation, Glucose Intolerance, and Insulin Resistance. Arterioscler Thromb Vasc Biol. 2016; 36:682–691. doi:10.1161/ATVBAHA.116.307166 [PubMed: 26868208]
42. Shimizu RT, Blank RS, Jervis R, Lawrenz-Smith SC, Owens GK. The smooth muscle alpha-actin gene promoter is differentially regulated in smooth muscle versus non-smooth muscle cells. J Biol Chem. 1995; 270:7631–7643. doi:10.1074/jbc.270.13.7631 [PubMed: 7706311]
43. Shirai H, Kidera A, Nakamura H. Structural classification of CDR-H3 in antibodies. FEBS Lett. 1996; 399:1–8. doi:10.1016/s0014-5793(96)01252-5 [PubMed: 8980108]
44. Abagyan R, Totrov M, Kuznetsov D. ICM? A new method for protein modeling and design: Applications to docking and structure prediction from the distorted native conformation. J Comput Chem. 1994; 15:488–506. doi:10.1002/jcc.540150503
45. Duewell P, Kono H, Rayner KJ, et al. NLRP3 inflammasomes are required for atherogenesis and activated by cholesterol crystals. Nature. 2010; 464:1357–1361. doi:10.1038/nature08938 [PubMed: 20428172]
46. Kadl A, Sharma PR, Chen W, et al. Oxidized phospholipid-induced inflammation is mediated by Toll-like receptor 2. Free Radic Biol Med. 2011; 51:1903–1909. doi:10.1016/j.freeradbiomed.2011.08.026 [PubMed: 21925592]
47. Tsimikas S, Brilakis ES, Lennon RJ, et al. Relationship of IgG and IgM autoantibodies to oxidized low density lipoprotein with coronary artery disease and cardiovascular events. J Lipid Res. 2007; 48:425–433. doi:10.1194/jlr.M600361-JLR200 [PubMed: 17093289]
48. Tsimikas S, Willeit P, Willeit J, et al. Oxidation-specific biomarkers, prospective 15-year cardiovascular and stroke outcomes, and net reclassification of cardiovascular events. J Am Coll Cardiol. 2012; 60:2218–2229. doi:10.1016/j.jacc.2012.08.979 [PubMed: 23122790]
49. Doran AC, Lehtinen AB, Meller N, et al. Id3 is a novel atheroprotective factor containing a functionally significant single-nucleotide polymorphism associated with intima-media thickness in humans. Circ Res. 2010; 106:1303–1311. doi:10.1161/CIRCRESAHA.109.210294 [PubMed: 20185798]
50. DeWitt WS, Lindau P, Snyder TM, et al. A Public Database of Memory and Naive B-Cell Receptor Sequences. PLoS One. 2016; 11:e0160853. doi:10.1371/journal.pone.0160853 [PubMed: 27513338]
51. Teplyakov A, Obmolova G, Malia TJ, et al. Structural diversity in a human antibody germline library. MAbs. 2016; 8:1045–1063. doi:10.1080/19420862.2016.1190060 [PubMed: 27210805]
52. Prohaska TA, Que X, Diehl CJ, et al. Massively Parallel Sequencing of Peritoneal and Splenic B Cell Repertoires Highlights Unique Properties of B-1 Cell Antibodies. J Immunol. 1 200:ji1700568. doi:10.4049/jimmunol.1700568
53. Yang Y, Wang C, Yang Q, et al. Distinct mechanisms define murine B cell lineage immunoglobulin heavy chain (IgH) repertoires. Elife. 2015; 4:e09083 doi:10.7554/eLife.09083 [PubMed: 26422511]
54. Regep C, Georges G, Shi J, Popovic B, Deane CM. The H3 loop of antibodies shows unique structural characteristics. Proteins. 2017; 85:1311–1318. doi:10.1002/prot.25291 [PubMed: 28342222]
55. Fellouse FA, Li B, Compaan DM, Peden AA, Hymowitz SG, Sidhu SS. Molecular recognition by a binary code. J Mol Biol. 2005; 348:1153–1162. doi:10.1016/j.jmb.2005.03.041 [PubMed: 15854651]
56. Fellouse FA, Barthelemy PA, Kelley RF, Sidhu SS. Tyrosine plays a dominant functional role in the paratope of a synthetic antibody derived from a four amino acid code. J Mol Biol. 2006; 357:100–114. doi:10.1016/j.jmb.2005.11.092 [PubMed: 16413576]

HIGHLIGHTS

- We generated a novel IgM autoantibody, 10C12, from the spleens of *Apoe*$^{-/-}$ mice fed a long-term Western diet that demonstrated specificity to the oxidized phospholipid, POVPC, in the Surface Plasmon Resonance assay and potent POVPC neutralizing activity *in vitro*.
- Preventive treatment with the 10C12 antibody inhibited the early inflammatory response in the abdominal lavage cells, as well as the early macrophage accumulation within arteries of *Apoe*$^{-/-}$ mice fed a short-term Western diet.
- In the intervention experiments, the 10C12 antibody did not alter preexisting atherosclerotic lesion pathogenesis in *Apoe*$^{-/-}$ mice fed a long-term Western diet with marked hyperlipidemia, but did decrease atherosclerosis in aged *sIgM*$^{-/-}$ *Apoe*$^{-/-}$ mice fed a standard low-fat diet with modest hyperlipidemia.

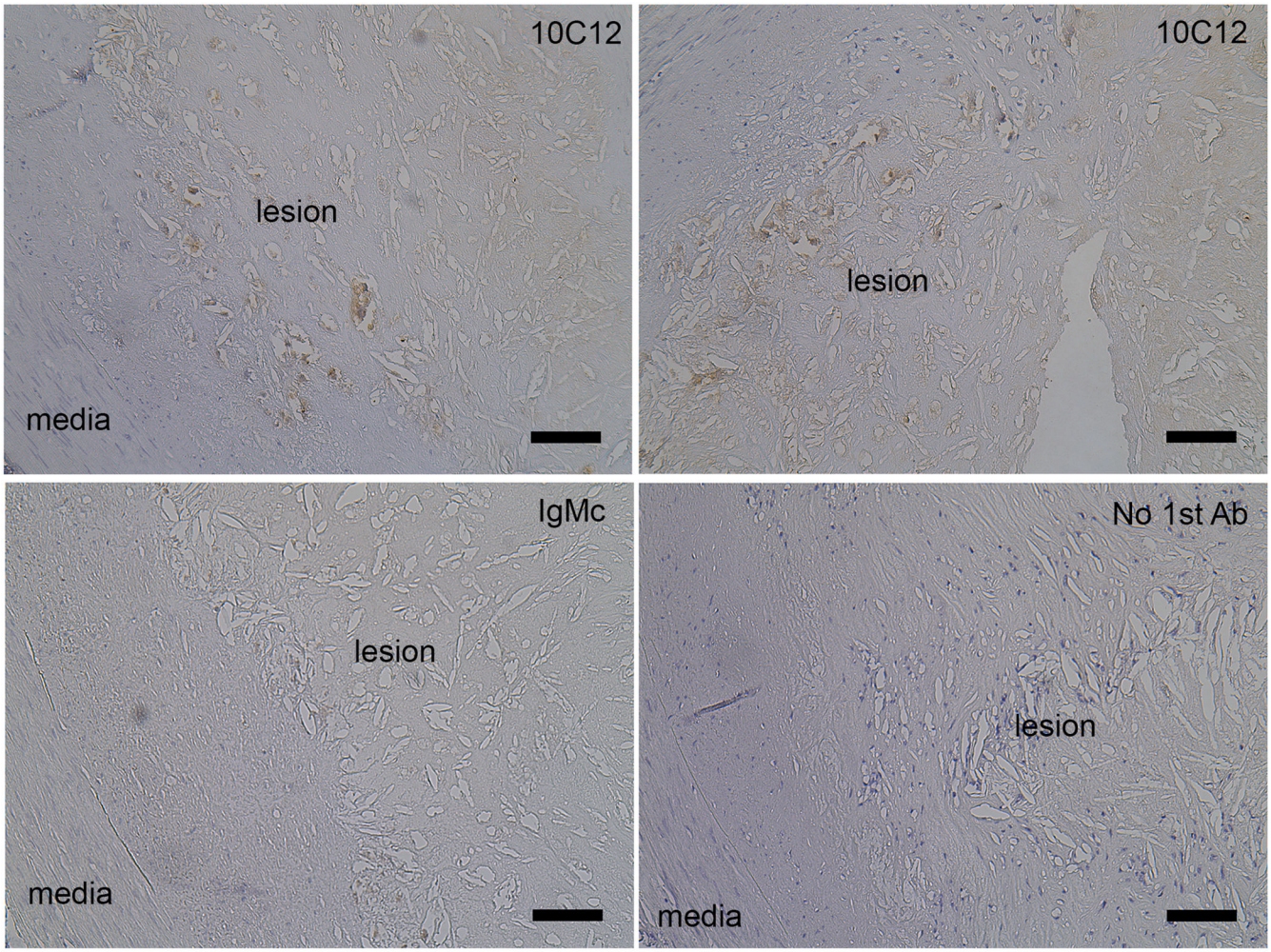

Figure 1. Human coronary artery atheromas exhibit 10C12 immunostaining.

Staining was done on 5 μm cross-sections of human autopsy samples using 10C12, IgM control antibody or only secondary antibody (no 1st Ab) followed by biotin-DAB visualization. Scale bar = 100 μm.

A

		Clone 10C12	Clone E06/T15
Light chain	CDR1	KASQDVGTAVA	TASESLYSSKHKVHYLA
	CDR2	WASTRHT	GASNRYI
	CDR3	QQYSSYPLT	AQFYSYPLT
Heavy chain	CDR1	GFSLTSYG	DFYME
	CDR2	IWSGGSTDYNAAFIS	SRNKANDYTTEYSASVKG
	CDR3	ARNGYYGSSWHYFDY	DYYGSSYWYFDV

B

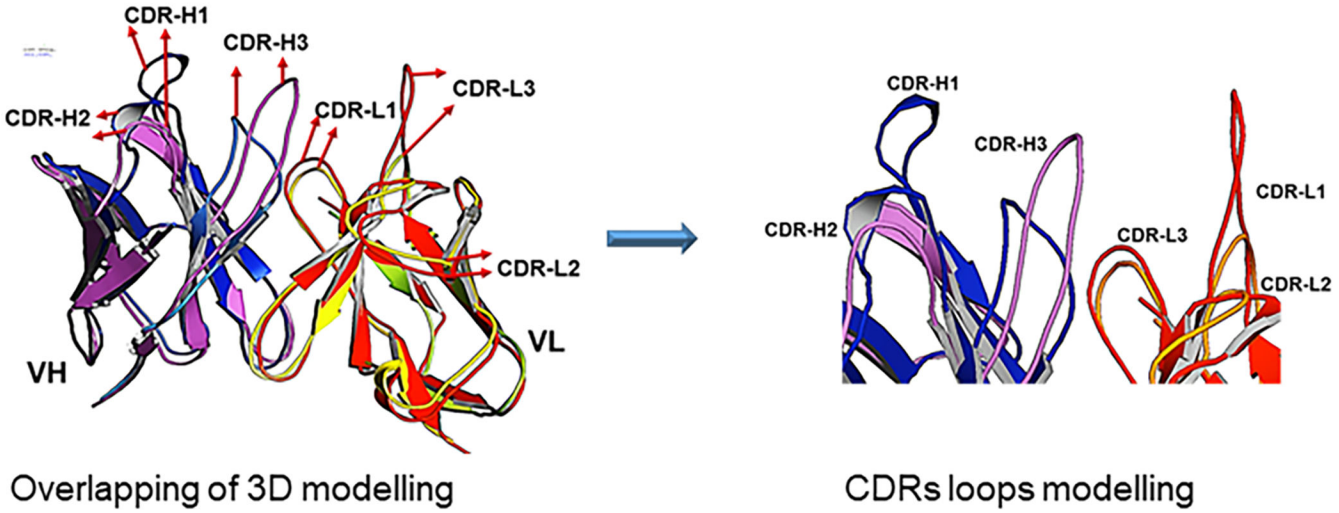

Figure 2. 10C12 and E06 are distinct anti-OxPL antibodies.

(A) Complimentary determining region (CDR) sequence alignment of 10C12 with E06 antibody. Amino acid sequences for the variable regions of the heavy chain (V_H) and light chain (V_L) of the 10C12 antibody and E06. (**B)** Predicted 3D structures of 10C12 and E06 single chain variable fragments (scFvs) with a comparison of the binding pockets. The V_H and V_L of 10C12 and E06 scFvs (**A**) are shown in a magnet of E06 V_H. Blue – 10C12 V_H, red – E06 V_L,and orange – 10C12 V_L, respectively.

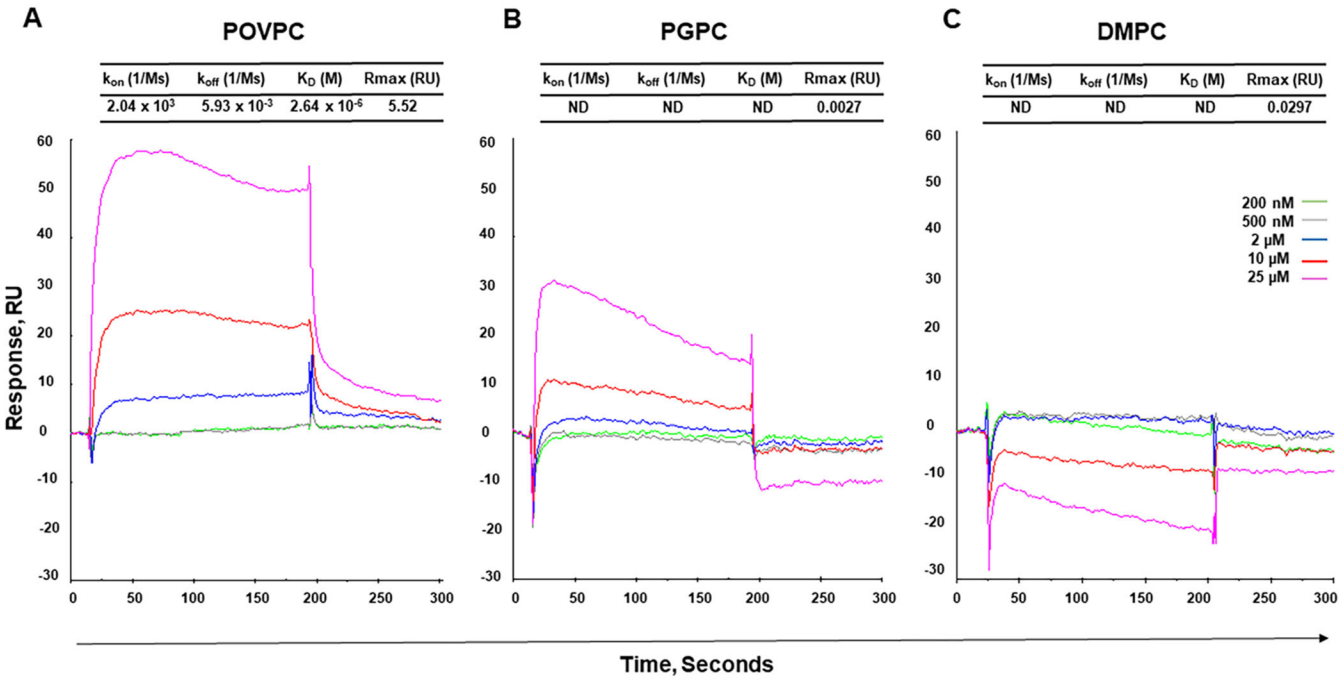

Figure 3. Surface Plasmon Resonance analysis of the 10C12 antibody interactions with phospholipids.

Sensograms of the interactions show association and disassociation phase as a relative response of SPR against time. (**A**) POVPC, (**B**) PGPC, (**C**) DMPC, (200 nM – 25 μM). Kinetic parameters obtained from the interactions of 10C12 with PLs. k_{on} – association constant; k_{off} – dissociation constant; K_D – equilibrium dissociation constant ($K_D = k_{off}/k_{on}$); R_{max} – the maximal feasible signal; RU – resonance units.

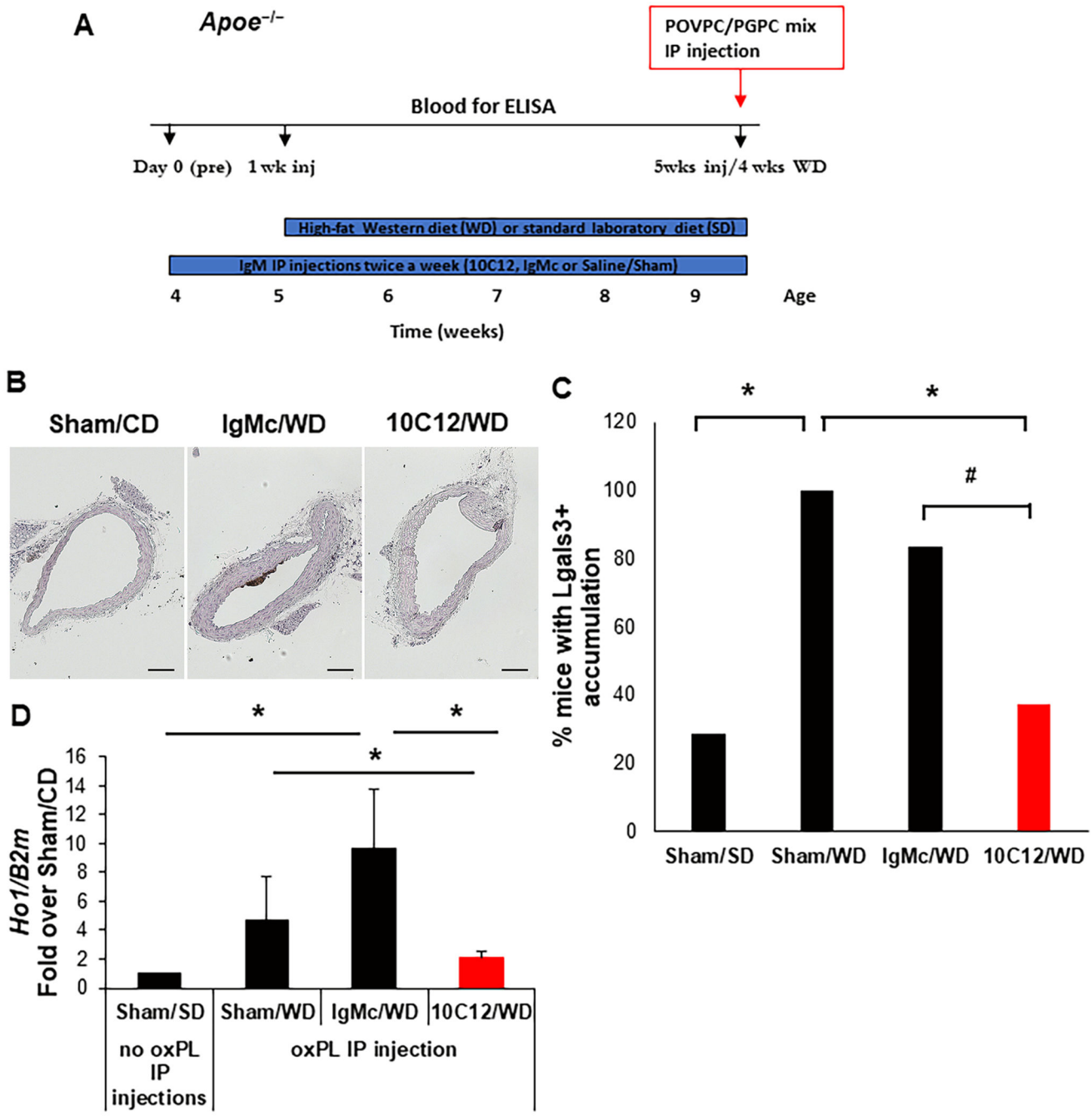

Figure 4. The 10C12 antibody inhibited the accumulation of LGALS3^{+} macrophages following 4-weeks of Western diet feeding of *Apoe*$^{-/-}$ mice.

(**A**) Four experimental groups were analyzed: Western diet plus IP injections with 10C12 IgM (10C12/WD, $n = 8$), IgM control (IgMc/WD, $n = 6$) or Saline/Sham (Sham/WD, $n = 5$); and standard laboratory low fat diet with Saline/Sham injections (Sham/SD, $n = 7$). To assess the efficacy of antibody treatments, 10C12/WD, IgMc/WD and Sham/WD mouse groups were injected IP with a 1:1 mixture of POVPC/PGPC (25 μg/25 μg) six hours before sacrifice. Abdominal lavage cells were collected and analyzed for the inflammatory

cytokines by qRT-PCR. Blood was collected for OxPL ELISA assays on days 0, 1 week, and 5 weeks as indicated by the schematic diagram. (**B**) 10C12 antibody treatment decreased the accumulation of $LGALS3^{+}$ cells in the brachiocephalic artery of $Apoe^{-/-}$ mice based on immunostaining (scale bar = 100 um). (**C**) The percentage of mice that have any LGALS3 positive staining within brachiocephalic arteries in each experimental group. Locations 45, 150 and 400 μm from aortic arch were analyzed for each animal. Mice were considered as LGALS3 positive if any of these three locations have LGALS3 positive staining; in other case, mice were considered as LGALS3 negative. Values = % LGALS3 positive mice per group. *P* values were calculated using a two-tail Fisher's exact test, $*P < 0.05$, $^{\#}P = 0.086$ (**D**) 10C12 antibody treatment decreased expression of the inflammatory marker *Ho1* in abdominal lavage cells after POVPC/PGPC IP injections. Results of qRT-PCR normalized to beta2-microglobulin (*B2m*) gene, means ± StDev, $*P < 0.05$ by Student's *t*-test.

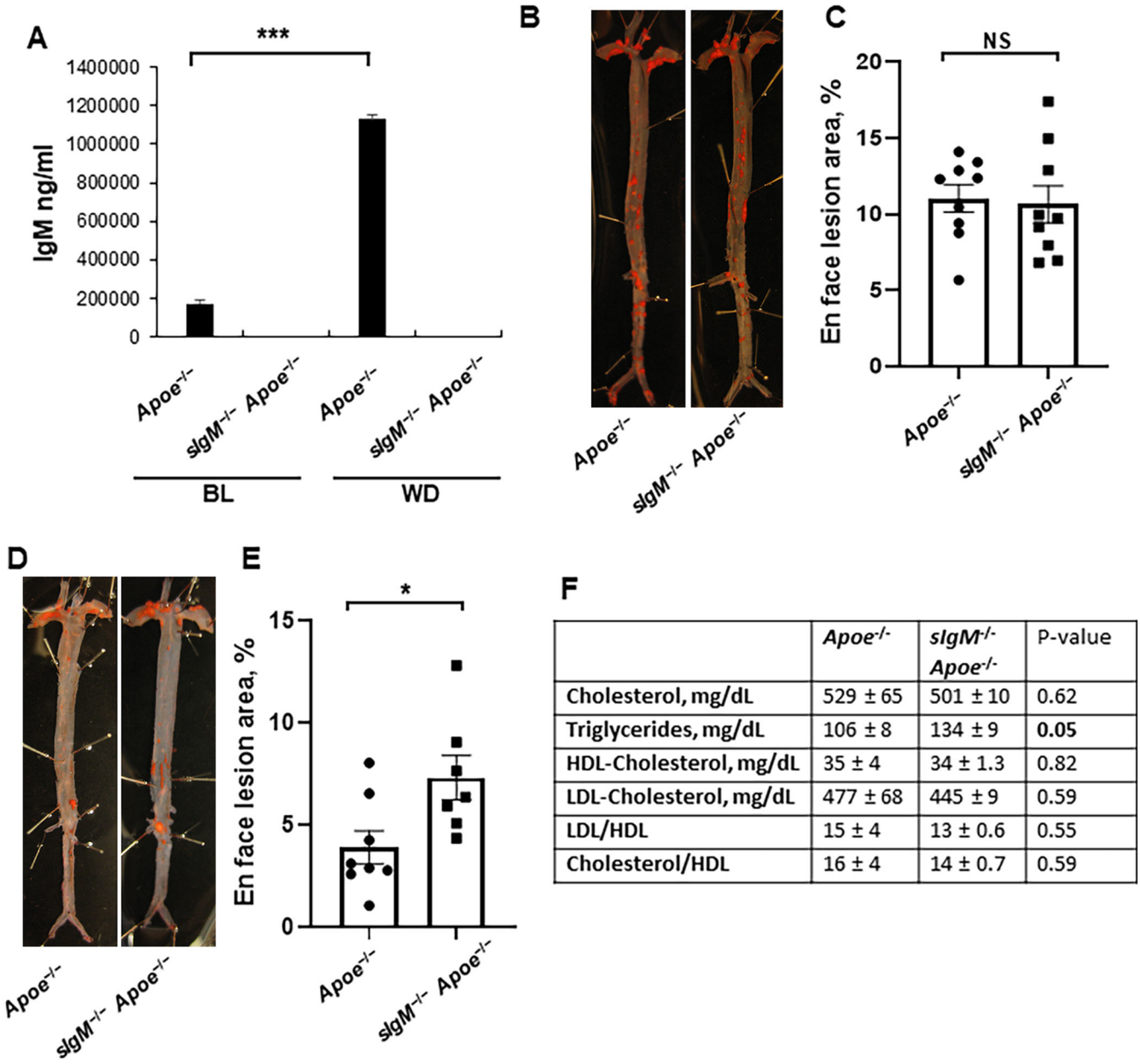

F

	Apoe$^{-/-}$	*sIgM*$^{-/-}$ *Apoe*$^{-/-}$	P-value
Cholesterol, mg/dL	529 ± 65	501 ± 10	0.62
Triglycerides, mg/dL	106 ± 8	134 ± 9	**0.05**
HDL-Cholesterol, mg/dL	35 ± 4	34 ± 1.3	0.82
LDL-Cholesterol, mg/dL	477 ± 68	445 ± 9	0.59
LDL/HDL	15 ± 4	13 ± 0.6	0.55
Cholesterol/HDL	16 ± 4	14 ± 0.7	0.59

Figure 5. Low fat diet-fed *sIgM* deficient *Apoe*$^{-/-}$ mice exhibited enhanced atherosclerosis.

(**A**) IgM levels in serum of *Apoe*$^{-/-}$ and *sIgM*$^{-/-}$*Apoe*$^{-/-}$ mice at baseline (BL) and after Western diet (WD) feeding. Values = mean ± SEM, n = 10 *Apoe*$^{-/-}$ BL, 10 *sIgM*$^{-/-}$ *Apoe*$^{-/-}$ BL, 7 *Apoe*$^{-/-}$ BL, 7 *sIgM*$^{-/-}$*Apoe*$^{-/-}$. (**B, C**) Sudan IV *en face* staining (**B**) and quantification (**C**) of lesion area in whole aorta of *Apoe*$^{-/-}$ and *sIgM*$^{-/-}$ *Apoe*$^{-/-}$ mice after 12 weeks of WD feeding. Values = mean ± SEM. (**D**,**E**) Sudan IV *en face* staining (**D**) and quantification (**E**) of lesion area in the whole aorta of standard laboratory diet-fed, 40 weeks old *Apoe*$^{-/-}$ and *sIgM*$^{-/-}$*Apoe*$^{-/-}$ mice. Values = mean ± SEM. *$P < 0.05$ and ***$P < 0.001$, data analyzed by Student's *t*-test. (**F**) Serum lipid profile analysis in standard laboratory diet-fed, 40 weeks old *Apoe*$^{-/-}$ and *sIgM*$^{-/-}$ *Apoe*$^{-/-}$ mice.

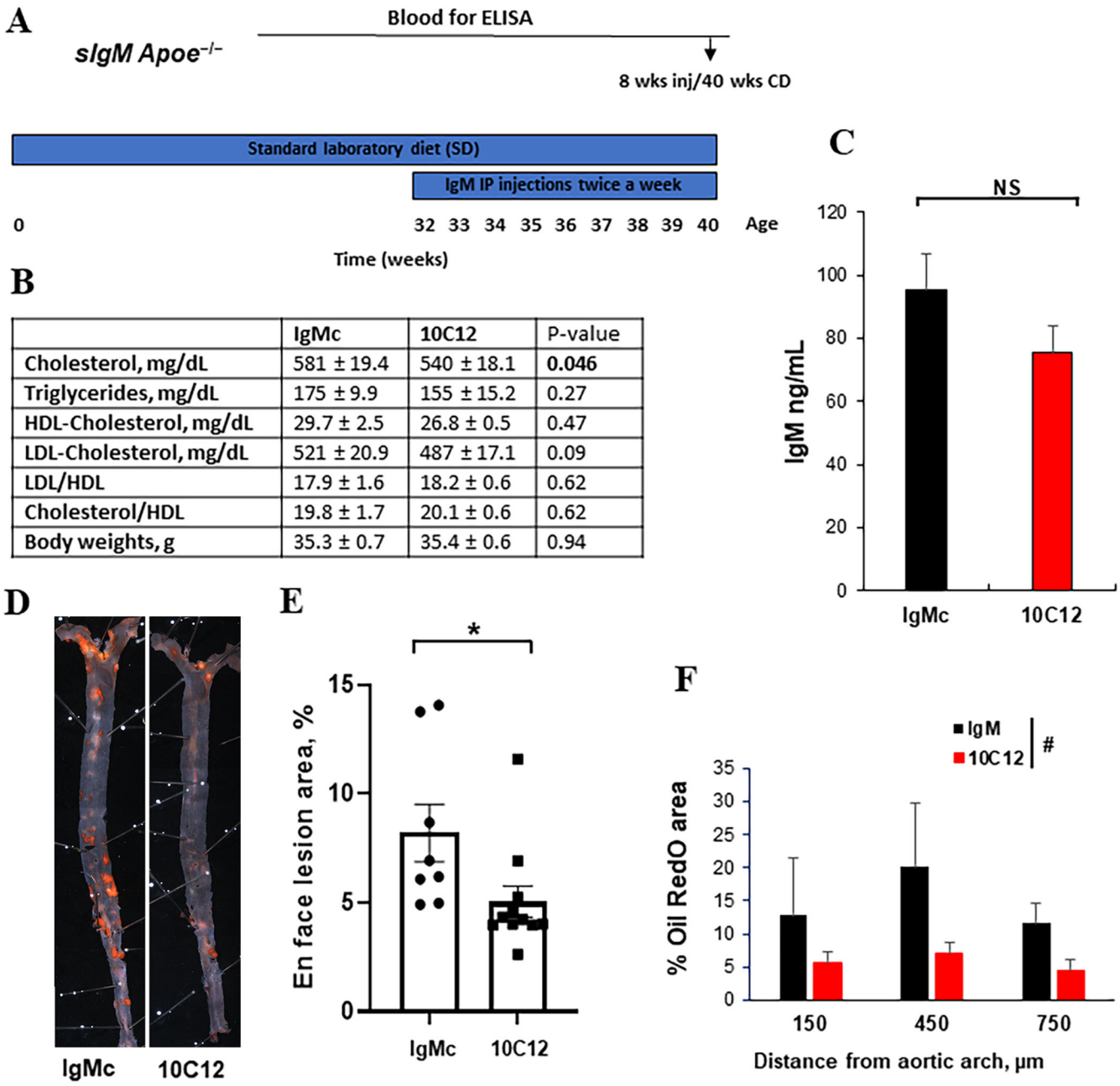

B	IgMc	10C12	P-value
Cholesterol, mg/dL	581 ± 19.4	540 ± 18.1	**0.046**
Triglycerides, mg/dL	175 ± 9.9	155 ± 15.2	0.27
HDL-Cholesterol, mg/dL	29.7 ± 2.5	26.8 ± 0.5	0.47
LDL-Cholesterol, mg/dL	521 ± 20.9	487 ± 17.1	0.09
LDL/HDL	17.9 ± 1.6	18.2 ± 0.6	0.62
Cholesterol/HDL	19.8 ± 1.7	20.1 ± 0.6	0.62
Body weights, g	35.3 ± 0.7	35.4 ± 0.6	0.94

Figure 6. The 10C12 antibody attenuated atherosclerosis development in low fat diet-fed *sIgM*$^{-/-}$*Apoe*$^{-/-}$ mice.

(**A**) Experimental design. *sIgM*$^{-/-}$ *Apoe*$^{-/-}$ mice were fed a low fat standard laboratory diet (SD) for 32 weeks. Between 32 – 40 weeks of age, mice were IP injected with 10C12 (n = 11) or IgM control (IgMc, n = 8) twice a week for 8 weeks. Arrows indicate when blood was collected for analyses. (**B**) Lipid profile and body weight analyses. Values = means ± SEM. (**C**) Mice treated with the 10C12 antibody and IgMc demonstrated equal IgM levels after eight weeks of injections based on IgM ELISA. NS – non significant by Student t-test. (**D**) Representative Sudan IV stained *en face* aorta preparations from *sIgM*$^{-/-}$ *Apoe*$^{-/-}$ mice treated with IgMc or 10C12. (**E**) 10C12 treated mice exhibited reduced Sudan IV positive

lesion area as compared to IgM treated control mice. Values = mean ± SEM. *$P < 0.05$ 10C12 versus IgMc by Mann-Whitney test. (**F**) Quantification of the percentage of lipid accumulation within the tunica media based on the Oil Red O staining of the cross-sections of atherosclerotic lesions within BCA of 10C12 treated mice compared to IgMc treated mice. Values represent mean ± SEM. $^{\#}P = 0.0582$ between treatments by 2-way ANOVA.

Table 1.

Detail results of the IMGT/V-QUEST analysis of V_H (heavy chain variable region) and V_L (light chain variable region) sequences of the 10C12 antibody.

Scores were calculated by +5 for each nucleotide that is identical to the IMGT reference sequence, and −4 for each mismatch. Identity indicates the percentage of nucleotides identical to the reference sequence, nt indicates a ratio of nucleotides identical to the reference sequence to the total number of nucleotides. (**A**) IMGT/V-QUEST analysis of V_H; (**B**) IMGT/V-QUEST analysis of V_L.

A			
Segment of 10C12 VH	**Gene and allele**	**Score**	**Identity % (nt)**
V	Musmus IGHV2-2*01 F	1420	identity = 100.00% (285/285 nt)
J	Musmus IGHJ2*01 F	235	identity = 100.00% (47/47 nt)
D	Musmus IGHD1-1*01 F	D-REGION is in reading frame 3	
B			
Segment of 10C12 VL	**Gene and allele**	**Score**	**Identity % (nt)**
V	Musmus IGKV6-23*01 F	1390	identity = 100.00% (279/279 nt)
J	Musmus IGKJ5*01 F	175	identity = 100.00% (35/35 nt)